

# Chemical Science

rsc.li/chemical-science



D  
R  
A  
G  
O  
N  
  
P  
O  
W  
E  
R

ISSN 2041-6539



## EDGE ARTICLE

Jerome Waser *et al.*

Fine-tuned organic photoredox catalysts for fragmentation-alkynylation cascades of cyclic oxime ethers



Cite this: *Chem. Sci.*, 2018, 9, 5883

Received 20th April 2018  
Accepted 28th May 2018

DOI: 10.1039/c8sc01818a

rsc.li/chemical-science

# Fine-tuned organic photoredox catalysts for fragmentation-alkynylation cascades of cyclic oxime ethers†

Franck Le Vaillant,<sup>a</sup> Marion Garreau,<sup>a</sup> Stefano Nicolai,<sup>a</sup> Ganna Gryn'ova,<sup>b</sup> Clemence Corminboeuf<sup>b</sup> and Jerome Waser<sup>\*a</sup>

Fine-tuned organic photoredox catalysts are introduced for the metal-free alkynylation of alkynitrile radicals generated *via* oxidative ring opening of cyclic alkylketone oxime ethers. The redox properties of the dyes were determined by both cyclic voltammetry and computation and covered an existing gap in the oxidation potential of photoredox organocatalysts.

## 1. Introduction

Cascade reactions leading to several bond forming/bond breaking events are important tools to access efficiently the complex carbon skeleton of organic compounds.<sup>1</sup> Single electron chemistry is well suited for cascade transformations due to the high reactivity of radical intermediates combined with neutral reaction conditions.<sup>2</sup> However, many radical-based cascade reactions still require the stoichiometric use of toxic reagents, such as tin hydrides and/or harsh reaction conditions. In the last decade, visible light driven photoredox catalysis has emerged as a general method for radical generation under mild oxidative or reductive conditions without the need for toxic reagents.<sup>3</sup> First successes were met with metal complexes as catalysts.<sup>4</sup> More recently organic dyes have been introduced, as they are often cheap, non-toxic and easy to modify.<sup>5</sup>

In the case of reductive quenching cycles for the generation of radical by oxidation, the reduction potential of the photo-activated catalyst is an essential parameter (Fig. 1). The reduction potential of the most often used iridium catalyst  $[\text{Ir}(\text{dF}(\text{CF}_3)\text{ppy})_2(\text{dtbbpy})]\text{PF}_6$  (**1**) (+1.21 V vs. SCE in MeCN)<sup>6</sup> is lower than frequently used organic dyes, such as Fukuzumi dye (**2**) and dicyanoanthracene (**3**) (+2.06 V vs. SCE in MeCN).<sup>5,7</sup> To enrich the range of transformations available to organic catalysts, using dyes with lower oxidation values would be highly desirable.

In this context, 2,4,5,6-tetra(9*H*-carbazol-9-yl)isophthalonitrile (4CzIPN, **4a**) has emerged as an alternative organic dye with a lower reduction potential (+1.35 V vs. SCE in MeCN).<sup>8</sup> Nevertheless, there is a need for further catalysts with reduction



Fig. 1 Bridging the gap in the reduction potential of activated organic photocatalysts.

<sup>a</sup>Laboratory of Catalysis and Organic Synthesis, Institut des Sciences et Ingénierie Chimique, Ecole Polytechnique Fédérale de Lausanne, CH-1015, Lausanne, Switzerland. E-mail: jerome.waser@epfl.ch

<sup>b</sup>Laboratory for Computational Molecular Design, Institut des Sciences et Ingénierie Chimique, Ecole Polytechnique Fédérale de Lausanne, CH-1015, Lausanne, Switzerland

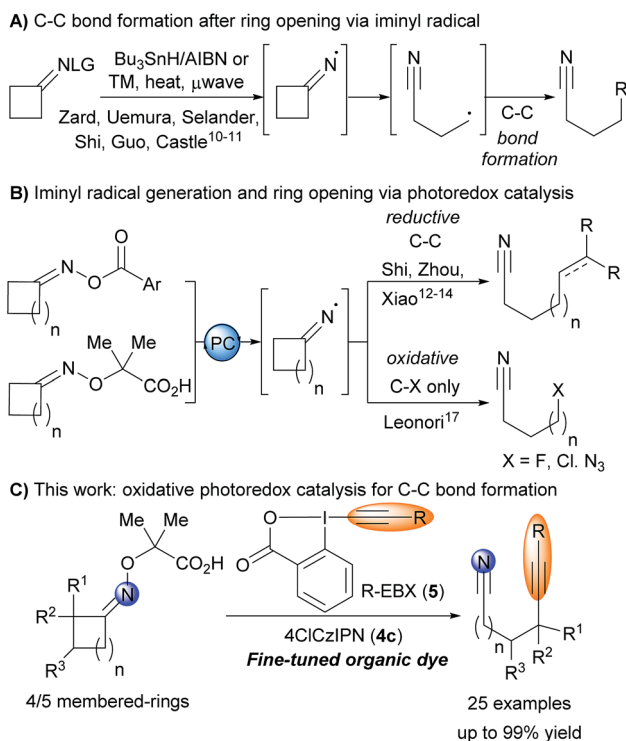
† Electronic supplementary information (ESI) available: Experimental and computational data. CCDC 1052646 and 1838186. For ESI and crystallographic data in CIF or other electronic format see DOI: 10.1039/c8sc01818a



potentials between +1.4 V and +2.0 V to allow challenging transformations asking for efficient oxidation.

In this context, heteroatom centered radicals initiated transpositions have found widespread applications in synthetic chemistry.<sup>9</sup> Zard and coworkers developed iminyl radical initiated cascades using tin reagents and electrophilic olefins to trap the generated intermediate (Scheme 1A).<sup>10</sup> Transition metal catalysis (Pd, Ir, Fe) and/or heating at temperature higher than 90 °C were later reported to avoid the use of tin reagents.<sup>11</sup> In 2017, Shi and co-workers described one single example of a Heck-like coupling at room temperature under photoredox conditions (Scheme 1B).<sup>12</sup> After Shi's pioneering example, Xiao and coworkers developed in 2018 a general method for C–C bond formation after reductive cleavage of cycloalkyloxime esters for the introduction of both alkanes and alkenes.<sup>13</sup> Zhou and coworkers reported a multicomponent alkylation etherification of alkenes using a similar strategy.<sup>14</sup> These breakthroughs greatly enhanced the synthetic potential of fragmentation cascades, but the exclusive use of reductive conditions limited the types of bond formations possible.

Recently, Studer and coworkers<sup>15</sup> and Leonori and coworkers<sup>16</sup> independently reported a new approach for the generation of iminyl radicals based on an oxidative quenching cycle starting from carboxylic acid derived oxime ethers. In 2018, this activation strategy was used by Leonori to develop the fluorination, chlorination and azidation of alkynitrile radicals generated by fragmentation of iminyl radicals (Scheme 1B).<sup>17</sup>



**Scheme 1** Existing methods for C–C bonds formation after iminyl radical initiated ring opening (A and B) and our work based on oxidative photoredox catalysis (C) (PC = photoredox catalysis, EBX = ethynyl benziodoxolone).

However, no example of C–C bond formation was reported. In this respect, our group and others have shown that ethynylbenziodoxolones (EBX) reagents **5** allowed the alkylation of radicals generated through oxidative photoredox cycles.<sup>18</sup> We therefore envisioned that EBX reagents would be ideally suited to overcome these limitations and deliver remotely-functionalized alkynyl nitrile through an oxidative fragmentation C–C bond formation sequence. Such a transformation has never been reported under photoredox conditions.<sup>19</sup> However, preliminary results showed that only low yields could be obtained in this reaction using established photoredox catalysts **1–3** (see Results and Discussions).

Herein, we report for the first time the use of the modified 4XCzIPN dyes **4b–d** in photoredox catalysis. In particular, 4ClCzIPN dye **4c** led to a highly efficient fragmentation alkylation process. Both theory and experiment showed that **4c** has an increased reduction potential compared to **4a**, leading to the efficient fragmentation of both four- and five-membered cyclic oxime ethers to give compounds containing versatile alkyne and nitrile functionalities in good yield under mild conditions.

## 2. Results and Discussions

### Dye synthesis and properties

The catalysts **4a–d** were easily synthesized from commercially available 2,4,5,6-tetrafluoroisophthalonitrile (**6**) and the corresponding carbazoles **7a–d** via nucleophilic aromatic substitution (Scheme 2).<sup>20</sup> Good yields were obtained, except for fluoro-substituted dye **4b**.

The redox properties of catalysts **4a–d** were then determined (Table 1). Ground state reduction and oxidation potentials of  $-1.21$  V and  $+1.52$  V for catalyst **4a** in acetonitrile have been reported based on cyclic voltammetry.<sup>8a</sup> These values combined with the difference in absorbance and emission signals of the dye allowed to estimate the potentials in the excited state:  $+1.35$  V and  $-1.04$  V for reduction and oxidation, respectively (entry 1). In our hand, slightly different values were obtained (entry 2). In particular, a higher reduction potential of  $+1.59$  V



**Scheme 2** Synthesis of 4XCzIPN dyes **4a–d**.





**Table 1** Literature (lit), measured (mes) and computed (comp) values for reduction potentials of dyes **4a–d**<sup>a</sup>

Entry	Catalyst	Solvent	$E_{1/2}(\text{P}/\text{P}^-)$	$E_{1/2}(\text{P}^+/\text{P})$	$E_{0-0}$	$E_{1/2}(\text{P}^*/\text{P}^-)$	$E_{1/2}(\text{P}^+/\text{P}^*)$
1	<b>4a</b> (lit)	CH <sub>3</sub> CN	−1.21	+1.52	2.56	+1.35	−1.04
2	<b>4a</b> (mes)	CH <sub>3</sub> CN	−1.05	+1.68	2.64	+1.59	−0.96
3	<b>4c</b> (mes)	CH <sub>3</sub> CN	−0.97	+2.05	2.68	+1.71	−0.63
4	<b>4a</b> (comp)	CH <sub>3</sub> CN	−1.29	+1.56	2.64 <sup>b</sup>	+1.35	−1.08
5	<b>4b</b> (comp)	CH <sub>3</sub> CN	−1.18	+1.67	—	—	—
6	<b>4c</b> (comp)	CH <sub>3</sub> CN	−1.10	+1.76	2.68 <sup>b</sup>	+1.58	−0.92
7	<b>4d</b> (comp)	CH <sub>3</sub> CN	−0.83	+1.89	2.65 <sup>b</sup>	+1.82	−0.76
8	<b>4a</b> (comp)	CH <sub>2</sub> Cl <sub>2</sub>	−1.29	+1.67	2.59 <sup>b</sup>	+1.30	−0.92
9	<b>4b</b> (comp)	CH <sub>2</sub> Cl <sub>2</sub>	−1.18	+1.79	2.60 <sup>b</sup>	+1.42	−0.81
10	<b>4c</b> (comp)	CH <sub>2</sub> Cl <sub>2</sub>	−1.10	+1.87	2.59 <sup>b</sup>	+1.49	−0.72
11	<b>4d</b> (comp)	CH <sub>2</sub> Cl <sub>2</sub>	−0.85	+1.98	2.58 <sup>b</sup>	+1.73	−0.60

<sup>a</sup> Potentials in V vs. SCE. The excitation energy  $E_{0-0}$  was estimated by the point of intersection of the normalized absorbance and emission signals.  $E_{1/2}(\text{P}^+/\text{P}^*) = E_{1/2}(\text{P}^+/\text{P}) - E_{0-0}$  and  $E_{1/2}(\text{P}^*/\text{P}^-) = E_{0-0} + E_{1/2}(\text{P}/\text{P}^-)$ . See ESI for details. <sup>b</sup> Experimental values of  $E_{0-0}$  were used.

was observed in the excited state. We then turned to halogenated dyes. With catalyst **4c**, both the cationic and anodic shifts were measured, with reduction and oxidation potentials of −0.97 V and +2.05 V (entry 3). This resulted in an increased reduction potential of +1.71 V of the photoexcited dye. Unfortunately, the cyclic voltammograms of dyes **4b** and **4d** could not be determined in acetonitrile due to their limited solubility. Only the absorption/emission spectra of dye **4d** could be measured. We therefore turned to theory to have a more reproducible and expanded access to redox potential values. At the PCM-UAKS/PBE0-D3BJ/def2-SVP level, the ground state reduction potentials decrease and the oxidation potentials increase in the order of **4a**, **4b**, **4c**, **4d** (entries 4–7).<sup>21</sup> This leads to a higher reduction potential in the excited state for catalyst **4c** and **4d** compared to **4a** (+1.58 V and +1.82 V respectively compared to +1.35 V). Therefore, both measurement and computation confirmed the increased potential for **4c**. The same trends but with lower reduction potentials were obtained in dichloromethane as solvent (entries 8–11). In this case, absorption and emission spectra could be measured for all dyes, but no good quality cyclic voltammograms could be acquired. Values in the ground state were therefore again obtained by computation.

The trend in reduction potentials increasing in the order of **4a** < **4b** < **4c** < **4d** (substituents on catalyst **4**: H < F < Cl < Br) can be rationalized as follows. Upon reduction, an electron is added to the lowest unoccupied molecular orbital (LUMO), located mostly on the central isophthalonitrile ring (Fig. 2). However, the LUMO also involves the carbazole moieties in the 4 and 6 positions of the isophthalonitrile ring and is potentially stabilized by them to a greater extent in the case of Cl and Br substituents (resonance donors) compared to H and F. We also note that while molecules **4a** and **4b** are fairly symmetric, systems **4c** and **4d** feature noticeable distortion of the 4-carbazole (Fig. 2). This peculiar structure, observed both in the gas-phase optimized geometries, obtained at several dispersion-corrected DFT levels, and experimental crystal structures,<sup>22</sup> is due to strong Cl⋯Cl and Br⋯Br contacts in **4c** and **4d**, respectively.<sup>23</sup>

### Optimization of the fragmentation cascade

Our investigations began with the gram scale synthesis of hydroxylamine **10** (Scheme 3, eqn (1)).<sup>24</sup> Nucleophilic substitution of commercially available *N*-hydroxyphthalimide (**8**) and ethyl 2-bromo-2-methylpropanoate (**9**), followed by acidic hydrolysis of the phthalimide, gave 5.8 g of **10** in 86% yield over 2 steps. Condensation of **10** with cyclobutanone (**11**) led to oxime ether **12a** in 90% yield as a crystalline solid (Scheme 3, eqn (2)).



**Fig. 2** Optimized structures and LUMO plots (isovalue 0.02) of the dyes **4a** and **4c** at the PBE0/def2-SVP level, as well as the crystal structure of **4c**. See the SI for the plots of **4b** and **4d**.





Scheme 3 Gram scale synthesis of 1-carboxy-1-methylethoxyammonium chloride (**10**), and condensation with cyclobutanone (**11**) to give model substrate **12a**.

A cyclic voltammetry measurement on the corresponding potassium carboxylate **12a'** showed a clear oxidation peak at +1.48 V vs. SCE in DMF. We decided then to first test the best catalysts reported by Studer:<sup>15</sup>  $[\text{Ir}(\text{dF}(\text{CF}_3)\text{ppy})_2(\text{dtbbpy})]\text{PF}_6$  (**1**) and Leonori:<sup>16,17</sup> Fukuzumi's catalyst **2** (Table 2). Based on our previous studies on photoredox catalysis using EBX reagents,<sup>18a,b</sup> we used DCE as solvent and an excess of Ph-EBX reagent **5a** (2.0 equiv.). With 1 mol% of **1a**, full conversion

and 55% NMR yield of alkyne **13a** were reached after 2 h, whereas only 50% conversion and 20% NMR yield was obtained with **2** (Table 2, entries 1–2). In both cases, significant side products formation was observed. DiCyanoAnthracene (DCA, **3**) gave only 5% NMR yield of **13a** (entry 3). With 4CzIPN (**4a**) we were pleased to observe 60% conversion of **12a** and 50% NMR yield of **13a** after 2 h (entry 4).

Increasing reaction time (6 h) and/or temperature (50 °C) was not successful to improve conversion. Speculating that stronger oxidizing dyes could lead to better results, catalyst **4c** was then examined. Full conversion of **12a** was observed and 70% of **13a** could be isolated (entry 5).  $\text{K}_2\text{CO}_3$  was found to be slightly better than  $\text{Cs}_2\text{CO}_3$  as a base (entry 6), allowing us to reduce the reaction time to 1 h (entry 7). The other new photocatalysts **4b** and **4d** were then tested, and provided similar photocatalytic activity as **4c** (entries 8–9). Due to its better solubility and ease of synthesis, **4c** was selected as photocatalyst to continue the study. Decreasing the number of equivalents of **5a** to 1.5 resulted in lower yield and more side reactions (entry 10). Interestingly, the catalyst loading could be decreased to 3 mol% (entry 11) or the reaction time reduced to only 30 min (entry 12) without any effect on the yield. Finally, control experiments showed that photocatalyst, base and light were all required for the reaction to proceed (entries 13–15).

Table 2 Optimization of the reaction conditions

The reaction scheme shows the conversion of model substrate **12a** (0.10 mmol) to alkyne **13a** using 2.0 equiv of Ph-EBX (**5a**) and 5 mol% of catalyst **1-4** in the presence of a base (1.1 equiv) in 0.05 M DCE at room temperature under blue LEDs.

Entry	Catalyst	Base	Time	Conversion <sup>a</sup>	Yield <sup>b</sup>
1 <sup>c,d</sup>	<b>1</b>	$\text{Cs}_2\text{CO}_3$	2 h	>95%	55%
2 <sup>d</sup>	<b>2</b>	$\text{Cs}_2\text{CO}_3$	2 h	50%	20%
3 <sup>d</sup>	<b>3</b>	$\text{Cs}_2\text{CO}_3$	2 h	90%	5%
4	<b>4a</b>	$\text{Cs}_2\text{CO}_3$	2 h–6 h	60%	50%
5	<b>4c</b>	$\text{Cs}_2\text{CO}_3$	2 h	>95%	70%
6	<b>4c</b>	$\text{K}_2\text{CO}_3$	2 h	>95%	75%
7	<b>4c</b>	$\text{K}_2\text{CO}_3$	1 h	>95%	80%
8	<b>4d</b>	$\text{K}_2\text{CO}_3$	1 h	>95%	75%
9	<b>4b</b>	$\text{K}_2\text{CO}_3$	1 h	>95%	75%
10 <sup>e</sup>	<b>4c</b>	$\text{K}_2\text{CO}_3$	1 h	>95%	70%
11 <sup>f</sup>	<b>4c</b>	$\text{K}_2\text{CO}_3$	1 h	>95%	80%
12	<b>4c</b>	$\text{K}_2\text{CO}_3$	0.5 h	>95%	80%
13	—	$\text{K}_2\text{CO}_3$	1 h	NR	NR
14	<b>4c</b>	—	1 h	<10%	5%
15 <sup>g</sup>	<b>4c</b>	$\text{K}_2\text{CO}_3$	1 h	NR	NR

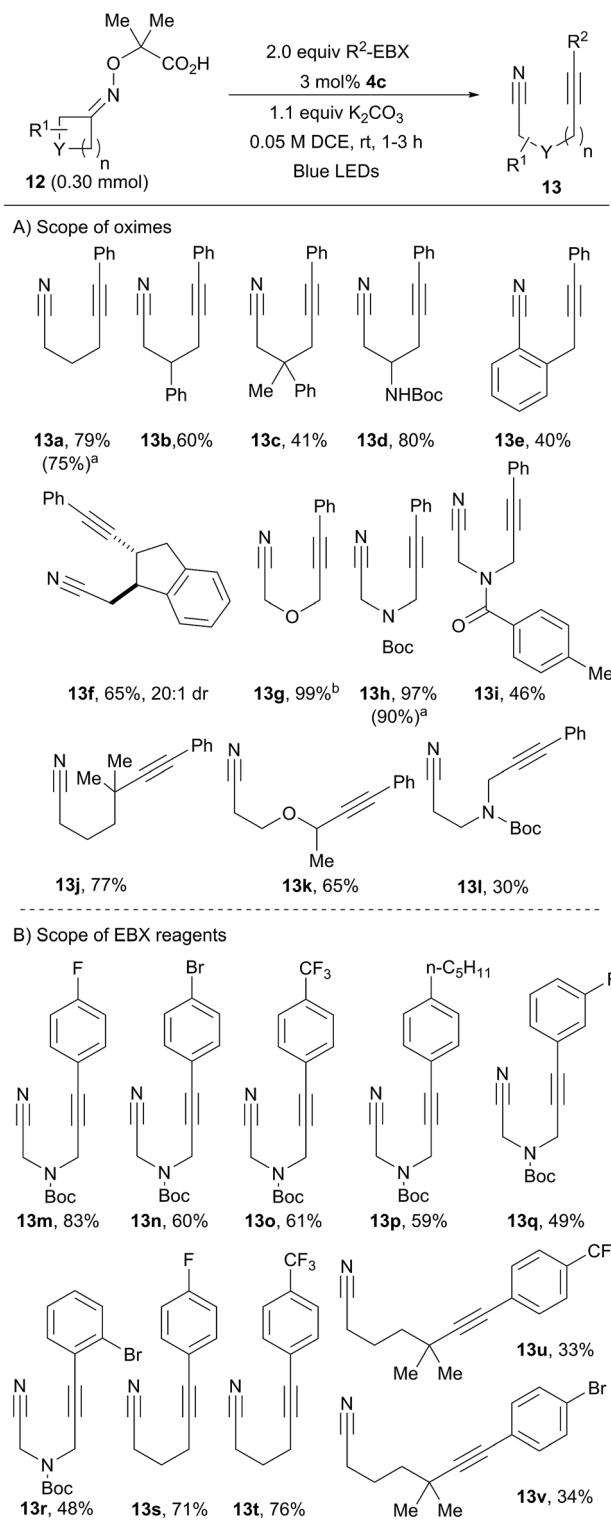
<sup>a</sup> Reaction conditions: using 0.1 mmol **12a** (1 equiv.), 0.2 mmol **5a** (2.0 equiv.), 5 mol% **1-4** (0.05 equiv.) in DCE (2.0 mL) for 2 h at RT. The conversion of **12a** by NMR is given. NR = no reactivity. <sup>b</sup> NMR yield using dibromomethane as internal standard. <sup>c</sup> Using 1 mol% of **1**. <sup>d</sup> Using 1.0 equiv. of base. <sup>e</sup> Using 1.5 equiv. of **5a**. <sup>f</sup> Using 3.0 mol% of organic dye **4c**. <sup>g</sup> Without irradiation.

### Scope of the fragmentation cascade

We then investigated the scope of oximes at 0.30 mmol scale using 3 mol% of **4c** (Scheme 4A). Oxime **12a** afforded **13a** in 79% isolated yield. Phenyl, alkyl and protected amines were tolerated at the  $\beta$ -position (**13b–d**, 41–80% yield). Benzocyclobutenone oxime **12e** afforded propargylic benzocarbonitrile **13e** in 40% yield. Bicyclic compound **13f** was obtained in 65% yield and excellent diastereoselectivity. Oxetanone and azetidinones oximes ethers were also excellent substrates (**13g–i**). Cyclopentanones derivatives were also successful. Using a *gem*-dimethyl substituent for the generation of a  $\delta$ -tertiary alkynitrile radical allowed the isolation of **13j** in 77% yield. In the work of Leonori and coworkers, a benzylic position was used to promote ring opening.<sup>17</sup> In our case, an  $\alpha$ -heteroatom was exploited. With an oxygen linker, product **13k** was obtained in 65% yield, whereas a nitrogen group led to a modest yield (30%) of **13l**. In addition, compounds **13a** and **13h** were obtained in similar yields using sunlight instead of LEDs.

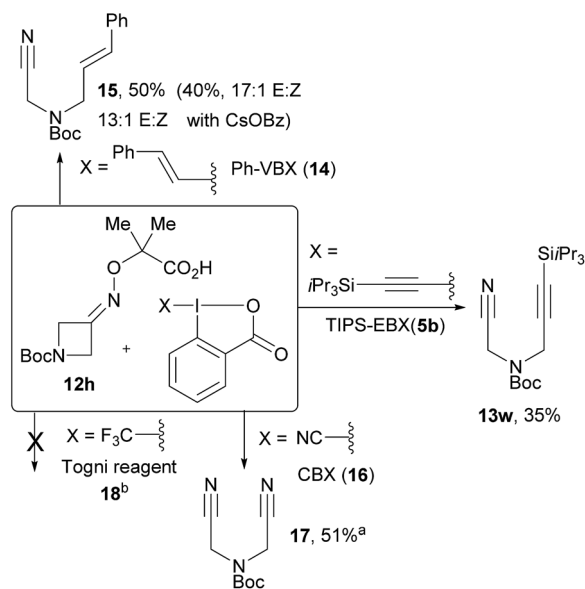
We then turned our attention to the scope of the reagents (Scheme 4B). The conversion of azetidinone oxime ether **12h** into  $\alpha$ - $\alpha'$ -cyanoalkynylamines was achieved in good yields, tolerating electron-withdrawing groups (**13m–o**) and electron-donating groups (**13p**) in *para* position of the benzene ring.<sup>25</sup> Good yields were also obtained with a fluorine in *meta* or a bromine in *ortho* positions (**13q** and **13r**). Cyclobutanone oxime **12a** could also be used with fluorinated arene substituents on the EBX (**13s–t**). Products **13u** and **13v** bearing a trifluoromethyl and bromine at the *para*-position were obtained in moderate yields from cyclopentanone oxime **12j**. Alkynyl nitriles are important building blocks combining two highly useful





**Scheme 4** Scope of the reaction. Using oximes **12** (1.0 equiv.), photocatalyst **4c** (3 mol%), EBX **5** (2 equiv.) and  $K_2CO_3$  (1.1 equiv.) in DCE (0.05 M) at rt, 1–3 h. <sup>a</sup>Using sunlight instead of blue LEDs. NMR yield is given. <sup>b</sup>On 0.10 mmol scale.

functional groups.<sup>26</sup> For example, compounds such as **13a** have been used in cyclization reactions with alkynes,<sup>26a–c</sup> vinyl iodonium salts,<sup>26d</sup> or benzyne equivalents.<sup>26e</sup>



**Scheme 5** Extension to other C–C bond forming reactions. Reaction conditions: 5 mol% **4c**,  $K_2CO_3$  (1.1 equiv.), 0.05 M DCE, blue LEDs, rt, 1 h. <sup>a</sup>Reaction run of reagent **16** (2 equiv.) for 14 h. NMR yield is given (isolated yield: 31%) <sup>b</sup>reaction run of reagent **18** (2 equiv.) for 24 h.

Preliminary investigations were then conducted for other types of C–C bond formation (Scheme 5). A silyl EBX reagent gave a lower yield of product **13w** and alkyl EBX could not be used. Preliminary results for an alkenylation cascade were also obtained using Phenyl Vinyl Benziodoxolone (PhVBX, **14**), recently introduced by Olofsson and co-workers.<sup>27</sup> Under the optimized reaction conditions, alkene **15** was isolated in 50% yield with a 12 : 1 *E/Z* selectivity.<sup>28</sup> Changing the base from  $K_2CO_3$  to CsOBz afforded lower yield (40%), but with enhanced selectivity (17 : 1 *E/Z*). Using two equivalents of cyanobenziodoxolone (CBX, **16**),<sup>18b</sup> bisnitrile **17** was obtained in 51% yield. With Togni reagent **18**,<sup>29</sup> no desired product was formed.

A one-pot protocol starting directly from the ketones was then developed (Scheme 6A). After condensation of cyclobutanone (**11**) with hydroxylamine **10**, addition of two equivalents of Ph-EBX (**5a**) and 5 mol% of the organic dye followed by one hour of irradiation delivered alkyne **13a** in 71% yield. A frequent drawback of organic dyes is their limited stability, leading often to low turnover numbers. Nevertheless, 66% of **13h** could still be isolated when using only 1 mol% of **4c** at a 1.0 mmol scale (Scheme 6B).

According to previous studies on EBX reagents,<sup>18a,b</sup> and the redox potential of dye **4c**, we assume that the reaction starts with the oxidation of the potassium carboxylate **12a'** ( $E_{1/2} = +1.48$  V vs. SCE in DMF) by the excited state  $PS^*$  of the organic dye to generate carboxyl radical **I** and the reduced state  $PS^-$  (Scheme 7). Fast decarboxylation releases the  $\alpha$ -oxy radical **II**, which can either lead to iminyl radical **III** after acetone extrusion, or can be directly trapped by EBX reagents forming **19**. Although **19** was not detected, its hydrated form **20** was observed by <sup>1</sup>H NMR. The iminyl radical **III** then fragments into a nucleophilic alkyl nitrile radical **IV**, which reacts with EBX 5.





Scheme 6 One-pot protocol and low catalyst loading.



Scheme 7 Speculative reaction mechanism.

For this step, a concerted mechanism *via* transition state TS1 can be envisioned according to our previous studies<sup>18b</sup> to afford the desired alkynyl nitrile and radical V. A  $\beta$ -addition followed by a 1,2 shift of the EBX substituent could also be considered depending on the migratory aptitude.<sup>18b</sup> Final reduction of V allows the regeneration of the ground state photocatalyst PS and generates carboxylate 21.

### 3. Conclusions

In summary, we have described the fine-tuning of organic dyes for the synthesis of alkynyl nitriles based on the alkynylation of alkynitrile radicals generated after a visible light-driven

oxidative ring fragmentation reaction involving an iminyl radical as intermediate. Preliminary results for the corresponding alkenylation and cyanation were also achieved. High yields were obtained in a short reaction time with low catalyst loading. We envision a bright future for these new dyes and further applications of cascade approaches in challenging C–C bond forming reactions.

### Conflicts of interest

There are no conflicts to declare.

### Acknowledgements

We thank ERC (European Research Council, Starting Grant iTools4MC, number 334840), the NCCR Chemical Biology (funded by the Swiss Science National Foundation) and EPFL for financial support. Ophélie Planes from the Laboratory of Supramolecular Chemistry at EPFL and Murat Alkan-Zambada and Laurent Liardet from the Laboratory of Inorganic Synthesis and Catalysis at EPFL are acknowledged for their help in the measurement of cyclic voltammograms. We thank Dr R. Scopelliti and Dr F. F. Tirani from ISIC at EPFL for X-ray analysis. G. G. acknowledges the funding from the European Union's Horizon 2020 research and innovation programme under the Marie Skłodowska-Curie grant agreement No. 701885.

### Notes and references

- (a) L. F. Tietze, *Chem. Rev.*, 1996, **96**, 115; (b) L. F. Tietze, G. Brasche and K. M. Gericke, *Domino Reactions in Organic Synthesis*, Wiley-VCH, 2006; (c) K. C. Nicolaou, D. J. Edmonds and P. G. Bulger, *Angew. Chem., Int. Ed.*, 2006, **45**, 7134.
- M. Yan, J. C. Lo, J. T. Edwards and P. S. Baran, *J. Am. Chem. Soc.*, 2016, **138**, 12692.
- (a) M. H. Shaw, J. Twilton and D. W. C. MacMillan, *J. Org. Chem.*, 2016, **81**, 6898; (b) D. W. C. Macmillan, C. R. J. Stephenson and T. P. Yoon, *Visible Light Photocatalysis in Organic Chemistry*, Wiley, 2018; (c) D. Ravelli, S. Protti and M. Fagnoni, *Chem. Rev.*, 2016, **116**, 9850.
- C. K. Prier, D. A. Rankic and D. W. C. MacMillan, *Chem. Rev.*, 2013, **113**, 5322.
- N. A. Romero and D. A. Nicewicz, *Chem. Rev.*, 2016, **116**, 10075.
- M. S. Lowry, J. I. Goldsmith, J. D. Slinker, R. Rohl, R. A. Pascal, G. G. Malliaras and S. Bernhard, *Chem. Mater.*, 2005, **17**, 5712.
- (a) S. Fukuzumi and K. Ohkubo, *Org. Biomol. Chem.*, 2014, **12**, 6059; (b) D. A. Nicewicz and T. M. Nguyen, *ACS Catal.*, 2014, **4**, 355; (c) C. Yang, J. D. Yang, Y. H. Li, X. Li and J. P. Cheng, *J. Org. Chem.*, 2016, **81**, 12357.
- (a) J. Luo and J. Zhang, *ACS Catal.*, 2016, **6**, 873; (b) J. K. Matsui and G. A. Molander, *Org. Lett.*, 2017, **19**, 436; (c) H. Huang, C. Yu, Y. Zhang, Y. Zhang, P. S. Mariano and W. Wang, *J. Am. Chem. Soc.*, 2017, **139**, 9799.





- 9 (a) S. Z. Zard, *Chem. Soc. Rev.*, 2008, **37**, 1603; (b) J. C. Walton, *Molecules*, 2016, **21**, 63.
- 10 (a) J. Boivin, E. Fouquet and S. Z. Zard, *J. Am. Chem. Soc.*, 1991, **113**, 1057; (b) J. Boivin, E. Fouquet and S. Z. Zard, *Tetrahedron*, 1994, **50**, 1757.
- 11 (a) T. Nishimura and S. Uemura, *J. Am. Chem. Soc.*, 2000, **122**, 12049; (b) T. Nishimura, Y. Nishiguchi, Y. Maeda and S. Uemura, *J. Org. Chem.*, 2004, **69**, 5342; (c) T. Nishimura, T. Yoshinaka, Y. Nishiguchi, Y. Maeda and S. Uemura, *Org. Lett.*, 2005, **7**, 2425; (d) H.-B. Yang and N. Selander, *Chem.-Eur. J.*, 2017, **23**, 1779; (e) Y.-R. Gu, X.-H. Duan, L. Yang and L.-N. Guo, *Org. Lett.*, 2017, **19**, 5908; (f) J. Wu, J.-Y. Zhang, P. Gao, S.-L. Xu and L.-N. Guo, *J. Org. Chem.*, 2018, **83**, 1046; (g) M. M. Jackman, S. Im, S. R. Bohman, C. C. L. Lo, A. L. Garrity and S. L. Castle, *Chem.-Eur. J.*, 2018, **24**, 594.
- 12 B. Zhao and Z. Shi, *Angew. Chem., Int. Ed.*, 2017, **56**, 12727.
- 13 X. Y. Yu, J. R. Chen, P. Z. Wang, M. N. Yang, D. Liang and W. J. Xiao, *Angew. Chem., Int. Ed.*, 2018, **57**, 738.
- 14 L. Li, H. Chen, M. Mei and L. Zhou, *Chem. Commun.*, 2017, **53**, 11544.
- 15 (a) H. Jiang and A. Studer, *Angew. Chem., Int. Ed.*, 2017, **56**, 12273; (b) H. Jiang and A. Studer, *Angew. Chem., Int. Ed.*, 2017, **57**, 1692.
- 16 J. Davies, N. S. Sheikh and D. Leonori, *Angew. Chem., Int. Ed.*, 2017, **56**, 13361.
- 17 E. M. Dauncey, S. P. Morcillo, J. J. Douglas, N. S. Sheikh and D. Leonori, *Angew. Chem., Int. Ed.*, 2018, **57**, 744.
- 18 (a) F. Le Vaillant, T. Courant and J. Waser, *Angew. Chem., Int. Ed.*, 2015, **54**, 11200; (b) F. Le Vaillant, M. D. Wodrich and J. Waser, *Chem. Sci.*, 2017, **8**, 1790; (c) Q.-Q. Zhou, W. Guo, W. Ding, X. Wu, X. Chen, L.-Q. Lu and W.-J. Xiao, *Angew. Chem., Int. Ed.*, 2015, **54**, 11196.
- 19 Castle and coworkers reported one single example of alkynylation in 54% yield using microwave irradiation at 90 °C and >3.5 equiv EBX reagent. See ref. 11g.
- 20 A. Kretzschmar, C. Patze, S. T. Schwaebel and U. H. F. Bunz, *J. Org. Chem.*, 2015, **80**, 9126. **4c** and **4d** were used for OLEDs applications in this work.
- 21 See the ESI† for computational methods.
- 22 (a) Crystal structure of **4a** is available at CCDC under number 1052646 (YUGDOV), see S. Wang, Y. Zhang, W. Chen, J. Wei, Y. Liu and Y. Wang, *Chem. Commun.*, 2015, **51**, 11972; (b) Crystal structure of **4c** is available at CCDC under number 1838186.
- 23 See the ESI† for a more detailed discussion.
- 24 **10** is commercially available at a high price from a limited number of suppliers. Its synthesis was described in the following patent, which is available only in Chinese: L. Jiang, J. Yang, Z. Shumin, Synthesis of Oxoamino-Aliphatic Carboxylic Acids, 1991, CN1051170 (A).
- 25 Aldehyde and nitrile substituents in *para* position of the ethynylarene were also tolerated, albeit led to low yield. (see ESI†).
- 26 (a) D. J. Brien, A. Naiman and K. P. C. Vollhardt, *J. Chem. Soc., Chem. Commun.*, 1982, 133; (b) J. A. Varela, L. Castedo and C. Saa, *J. Am. Chem. Soc.*, 1998, **120**, 12147; (c) L.-G. Xie, S. Shaaban, X. Chen and N. Maulide, *Angew. Chem., Int. Ed.*, 2016, **55**, 12864; (d) J. Sheng, Y. Wang, X. Su, R. He and C. Chen, *Angew. Chem., Int. Ed.*, 2017, **56**, 4824; (e) Y. Wang, C. Chen, S. Zhang, Z. Lou, X. Su, L. Wen and M. Li, *Org. Lett.*, 2013, **15**, 4794.
- 27 (a) E. Stridfeldt, A. Seemann, M. J. Bouma, C. Dey, A. Ertan and B. Olofsson, *Chem.-Eur. J.*, 2016, **22**, 16066; (b) A. Boelke, L. D. Caspers and B. J. Nachtsheim, *Org. Lett.*, 2017, **19**, 5344.
- 28 Ph-VBX was first used in photoredox catalysis by Leonori and coworkers (see ref. 16), affording only the *E* isomer.
- 29 (a) P. Eisenberger, S. Gischig and A. Togni, *Chem.-Eur. J.*, 2006, **12**, 2579; (b) J. Charpentier, N. Frueh and A. Togni, *Chem. Rev.*, 2015, **115**, 650.

